Proc. Indian Acad. Sci. (Earth Planet. Sci.), Vol. 103, No. 2, June 1994, pp. 107–123.

Circulation and water masses of the Arabian Sea

S R SHETYE, A D GOUVEIA and S S C SHENOI

Physical Oceanography Division, National Institute of Oceanography, Dona-Paula, Goa 403 004, India

Abstract. The dynamics and thermodynamics of the surface layer of the Arabian Sea, north of about 10 N, are dominated by the monsoon-related annual cycle of air-sea fluxes of momentum and heat. The currents in open-sea regime of this layer can be largely accounted for by Ekman drift and the thermal field is dominated by local heat fluxes. The geostrophic currents in open-sea subsurface regime also show a seasonal cycle and there is some evidence that signatures of this cycle appear as deep as 1000 m. The forcing due to Ekman suction is an important mechanism for the geostrophic currents in the central and western parts of the Sea. Recent studies suggest that the eastern part is strongly influenced by the Rossby waves radiated by the Kelvin waves propagating along the west coast of India.

The circulation in the coastal region off Oman is driven mainly by local winds and there is no remotely driven western boundary current. Local wind-driving is also important to the coastal circulation off western India during the southwest monsoon but not during the northeast monsoon when a strong (approximately 7×10^6 m^3/sec) current moves poleward against weak winds. This current is driven by a pressure gradient which forms along this coast during the northeast monsoon due to either thermohaline-forcing or due to the arrival of Kelvin waves from the Bay of Bengal.

The present speculation about flow of bottom water (deeper than about 3500 m) in the Arabian Sea is that it moves northward and upwells into the layer of North Indian Deep Water (approximately 1500–3500 m). It is further speculated that the flow in this layer consists of a poleward western boundary current and a weak equatorward flow in the interior. It is not known if there is an annual cycle associated with the deep and the bottom water circulation.

Keywords. Arabian Sea; N. Indian Ocean; water masses; mixed layer; circulation; coastal currents.

1. Introduction

Two features stand out in distinguishing the N. Indian Ocean from other oceans. First, the northernmost extent of its poleward boundary is close to 25 N, making it essentially a tropical ocean. Second, the occurrence of the southwest and the northeast monsoon over the ocean implies that the winds are strongly seasonal. Seasonal variation of such a large amplitude is generally not found elsewhere. The N. Indian Ocean can be divided roughly into three major areas: the equatorial belt stretching between 10 N and 10 S, with the Somalia basin on its western end; the Bay of Bengal; and, the Arabian Sea. Of the three areas, the Somalia basin has been the best studied from the point of view of both observations and theory. Schott (1983) provides a review of the observations. Luther and O'Brien (1985) have discussed the theoretical issues concerning the circulation in the Somalia basin. The rest of the equatorial belt is poorly observed. The Bay of Bengal stretches north of about 10 N and east of about 80 E. Some of the recent studies describing the circulation in the Bay are Shetye *et al* (1991b), Murty *et al* (1992) and Shetye *et al* (1993). The dynamics of the circulation

of the Bay of Bengal has been discussed in Potemra *et al* (1991), Yu *et al* (1991) and McCreary *et al* (1993). The purpose of this review is to outline salient features of the large-scale circulation and water masses of the Arabian Sea.

Robinson (1966), quoting the International Hydrographic Bureau (Sp. Publ. 23, 1953), defines the southern boundary of the Arabian Sea (figure 1) by a line from Ras Hafun (Somalia, 10·29 N 51·20 E) to Addu Atoll (approximately 73·25 E 0·58 S), up the western edge of the Maldives and Lakshadweep, to Sadashivgad Light on the west coast of India (14·80 N). The Gulf of Aden is separated by the meridian of Ras Asir (Somalia, 51·25 E), and the Gulf of Oman by a line from Ras Limah (25·95 N) in Oman to Ras al Kuh (Iran, 25·80 N). In this paper we restrict our attention to the region north of approximately 8 N. The region off Somalia has not been included in the discussion because, as pointed out earlier, the circulation and water masses of this region have been examined in quite a few papers.

The following are the main characteristics of bottom topography in the Arabian Sea. The northwest-southeast oriented Carlsberg Ridge is located in the southern part of the Arabian Sea. The southwest-northeast oriented Murray Ridge is in the north. In the mid-Arabian Sea there is a topographic slope: depth shoals from 4000 m to 3000 m from 14 N to 21 N. The continental shelf, as marked by the 200 m contour (figure 1), is approximately 120 km wide off the southern tip of India, narrows to about 60 km off 11 N and widens to about 350 km off the Gulf of Cambay. The shelf remains about 200 km wide as far north as Karachi, west of which the shelf narrows to less than 50 km. The shelf is narrow all along the Arabian coast and is less than 50 km wide at the entrance of the Red Sea.

The Arabian Sea is thus an approximately triangular basin with the largest zonal extent of about 3000 km and a slightly smaller meridional extent. Its proximity to the equator makes the radius of deformation to be about 100 km. We take the coastal regime of the Arabian Sea, as against the open-sea regime, to be a belt of width of

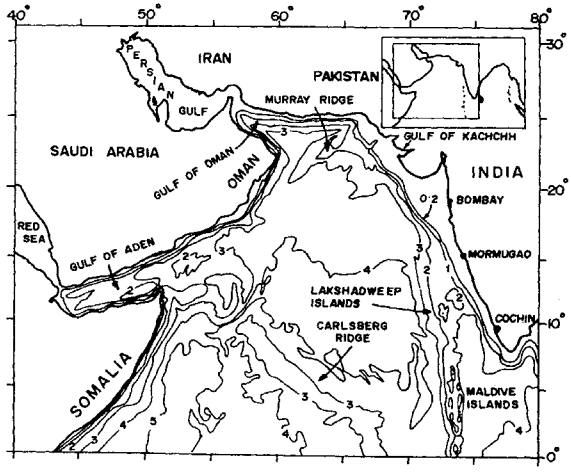

Figure 1. The Arabian Sea. The bottom topography contours are in kms.

a couple of radii of deformation from coastline. The small size of the Arabian Sea (relative to the Atlantic, Pacific, and south Indian Ocean basins) implies that its coastal regime, stretched along two sides of the triangular basin, occupies a good fraction, about 25%, of total area. It is expected that interaction between the open-sea and the coastal regime is important to the dynamics of the Sea. Crucial to the understanding of its dynamics and thermodynamics are the monsoon winds which are described in the next section. Prominent features of the circulation in the Sea are discussed in section 3, first for the open-sea regime then for the coastal regime. Section 4 examines mixed-layer processes in the Sea and characteristics of the water masses are reviewed in section 5.

2. Wind stress distribution

The annual cycle of stress exerted by monsoon winds at the surface of the Arabian Sea is shown in figure 2 using the monthly wind stress climatology of Hellermann and Rosenstien (1983). The winds blow strongly during May–September, the southwest monsoon, forming the Findlater Jet with maximum wind stress magnitudes of about 6 dyne/cm^2. The winds during this season are generally from the southwest, however, they are approximately from the west off the southern part of west coast of India. During the northeast monsoon, November–February, the winds blow from the northeast and have maximum wind stress magnitudes of about 2 dyne/cm^2. March–April and October are transition months and winds are weak.

The dominant period in wind stress variability due to the monsoons is one year. This was brought out by Breidenbach (1990) who examined the EOFs of the pseudo-stress over the Indian Ocean during 1977–85. It was found that the first EOF, which accounted for 65·5% of the variance, had a period of a year and its spatial pattern was related to the monsoon circulation. The second, third and fourth EOFs accounted for, respectively, 5·8%, 3·2% and 2·9% of the variance. We can therefore look at the Arabian Sea winds as being of predominantly annual period.

3. Velocity field

The only data set that at the present can give a comprehensive description of surface velocity field in the N. Indian Ocean is climatology of ship-drifts. Cutler and Swallow (1984) have compiled 10-day averages of historical ship-drift data on 1° × 1° grid in the Indian Ocean between latitudes 25 S and 20 N. Figure 3 shows the field of monthly ship-drifts in the Arabian Sea derived from the Cutler and Swallow data. As seen from the figure, surface currents are approximately clockwise during the southwest monsoon; northeastward in the west, eastward in the mid-sea and southeastward in the east. They are counter-clockwise and weaker during the northeast monsoon. To examine the causes behind the features seen in figure 3, and to study the subsurface flow, it is useful to divide the basin into two regimes – open sea and coastal.

3.1 *Open-sea regime*

The eastward surface flow in the central Arabian Sea during May–October seen in

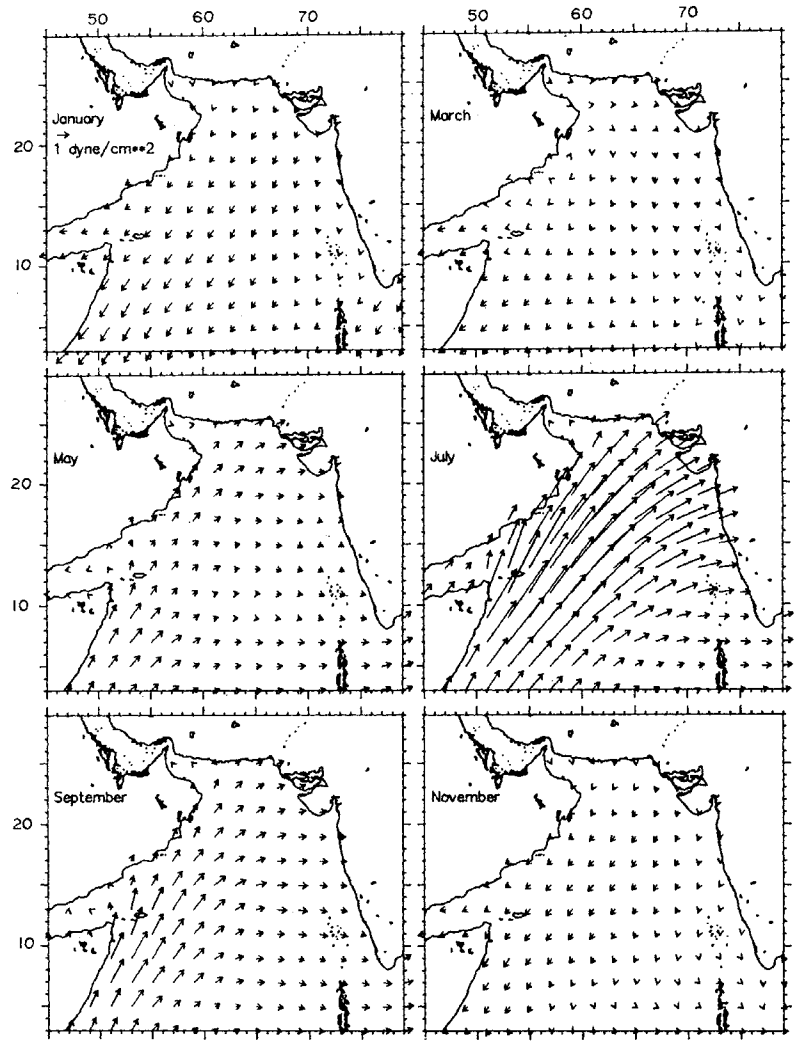

Figure 2. Annual cycle of wind stress over the Arabian Sea. Data are from Hellermann and Rosenstien (1983). Month is given in the upper left hand corner of each box. The vector shown just below the month January represents 1 dyne/cm^2.

figure 3 is fed by a strong northeastward surface flow from the Somali basin which at this time has an energetic coastal current (Schott 1983). The westward drift during November–February is part of a general movement in that direction during the northeast monsoon over the entire N. Indian Ocean basin north of the equator (Wyrtki 1973).

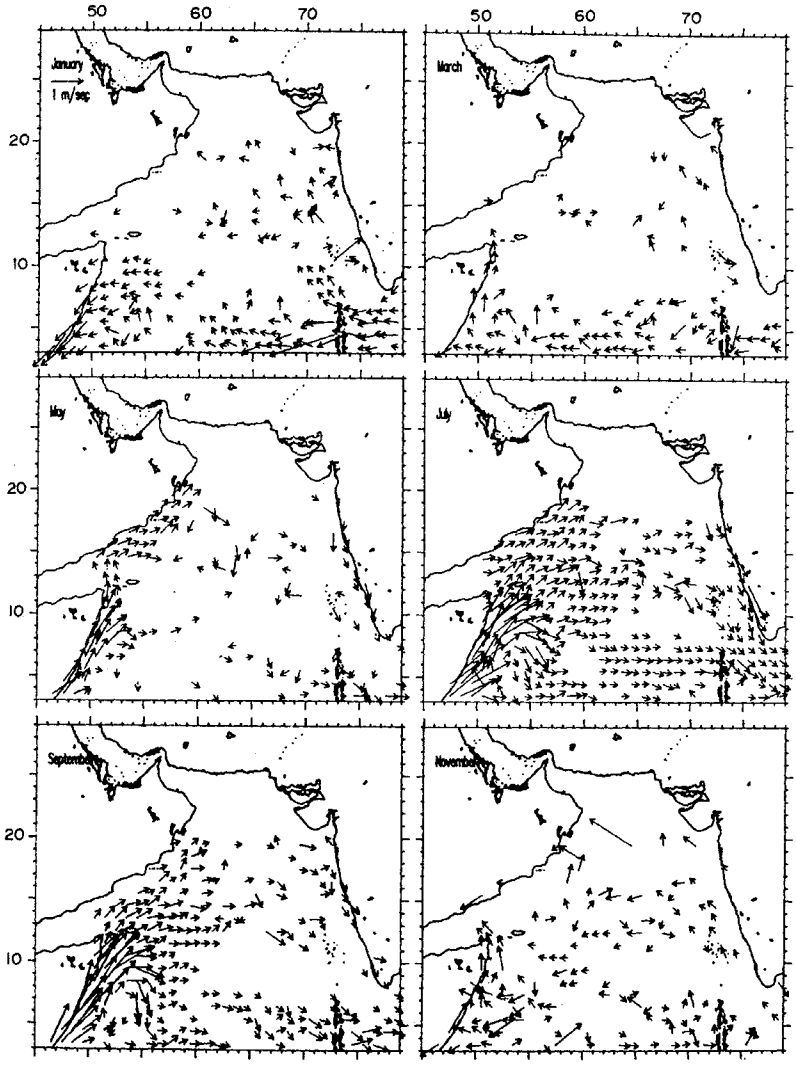

Figure 3. Annual cycle of ship-drifts in the Arabian Sea. The scale shown in the upper left hand corner of the January figure applies to the vectors in figures for other months as well. The 10-day climatology of ship-drifts compiled by Cutler and Swallow (1984) was used. Ten-day drifts over three consecutive 10-day periods at a location were averaged to construct the monthly-mean drift at the location; in computation of the average, the number of observations that go into each 10-day ship-drift vector were noted. January (June) represents the average during Julian days 1–30 (151–180). To avoid clutter monthly ship-drifts less than 20 cm/sec are not plotted. The Cutler and Swallow data do not cover region north of 20 N.

To study dynamics of surface currents, Hastenrath and Greischar (1991) compared monthly ship-drifts with the Ekman drifts computed from the fields of monthly wind stress and with the surface geostrophic velocity estimated from dynamic topography (0/400) for a few regions in the open-sea regime of the Indian Ocean. One such region covers a portion of the southeastern part of the Arabian Sea (2–10 N, 60–80 E). Under the influence of monsoon winds the Ekman flow in this region is directed south of the east during the southwest monsoon and in opposite direction during the northeast monsoon. Hastenrath and Greischar concluded that in comparison to the Ekman velocity, the geostrophic velocity at surface is weak throughout the year. It is eastward during the southwest monsoon and westward during the northeast monsoon. The observed surface current differs little from the sum of the calculated Ekman and geostrophic components. Transports due to both Ekman and geostrophic flow were found to be weak. The annual mean of geostrophic transport was found to be $3 \times 10^6 m^3/s$ towards the west. On the whole, the analysis suggests that the surface velocity field in the Arabian Sea is primarily due to wind-driven Ekman flow. It is strongly seasonal, shallow, and overrides a weaker seasonally varying geostrophic flow. Though analysis similar to the above has not been carried out over the whole of the Arabian Sea, there is other evidence to believe that wind forcing dominates near surface processes in the open Arabian Sea (see section 4).

Pattern of geostrophic flow can be inferred from dynamic topography. In figures 4,

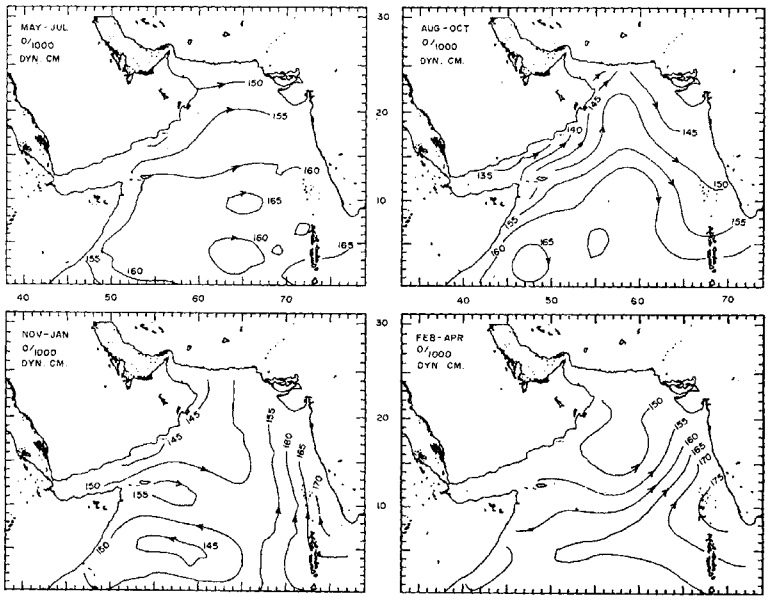

Figure 4. Dynamic topography of the surface w.r.t. 1000 db during different seasons using the one-degree temperature and salinity profiles given in Levitus (1982) atlas.

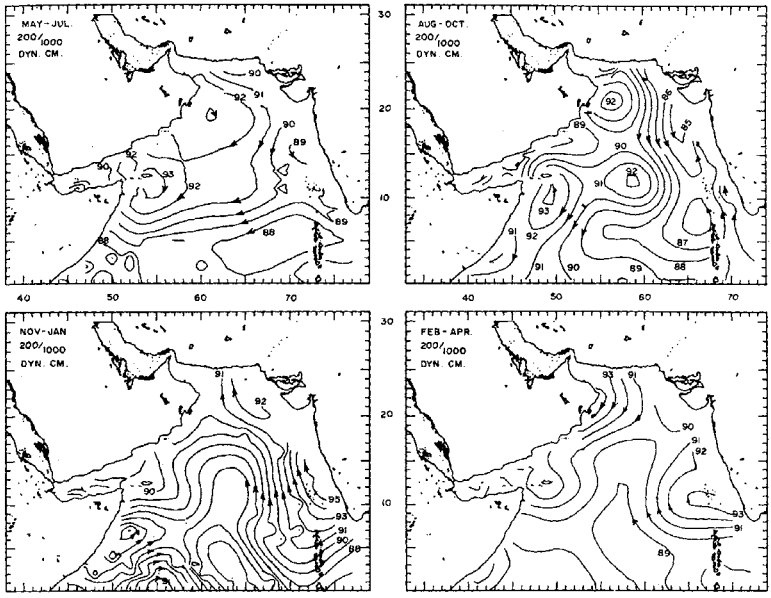

Figure 5. Same as in figure 4 but 200 db.

5, and 6 we have constructed the dynamic topography at surface, 200 m, and 500 m, respectively, using the seasonal temperature and salinity data from Levitus (1982) atlas which has spatial resolution of 1° × 1°. The surface geostrophic flow during May–October is eastward (figure 4). It is stronger during the later half of this period when the flow also has a northward component in the western part of the Sea and a southward flow in the eastern part. With onset of the northeast monsoon, the circulation in the Arabian Sea reverses. During November–January the most prominent feature in surface geostrophic flow is a poleward current in the eastern part of the basin. As we see in section 3.2, this flow matches with a strong poleward coastal current along the west coast of India during this season. The pattern of circulation at 200 m (figure 5) is more complicated than that at surface and has cellular structures reminiscent of the dynamic topographies given by Duing (1970). During the southwest monsoon, particularly during its second half, there are suggestions of a poleward undercurrent in the coastal region off southwest India. As seen later, this is consistent with the pattern inferred from hydrographic data collected in the coastal region of India. The circulation at 200 m is best developed during the northeast monsoon when an anti-clockwise flow exists with a poleward flow in the eastern half of the basin and an equatorward flow in the western half. During February–April, the transition period between the northeast and the southwest monsoon, a similar pattern exists but the magnitude is weaker. The pattern of geostrophic circulation at 500 m (figure 6) mimics that at 200 m but is much weaker.

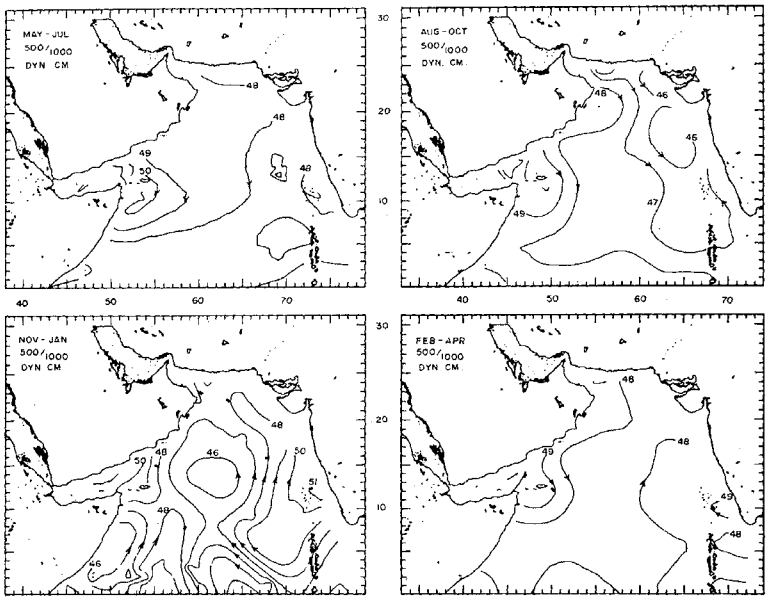

Figure 6. Same as in figure 4 but 500 db.

The results of recent numerical experiments with a reduced gravity $2^1/2$-layer model by McCreary *et al* (1993) suggest that Ekman suction is important to the interior flow in the central and western parts of the Arabian Sea. The numerical experiments further suggest that Ekman suction is not important to behaviour of the geostrophic flow in the eastern part of the Arabian Sea. Instead, McCreary *et al* suggest that the coastal Kelvin waves moving poleward along the west coast of India radiate westward propagating Rossby waves which strongly influence the velocity field in the eastern part. In these numerical experiments some of the Kelvin waves originate in the Bay of Bengal and travel along the coasts of India and Sri Lanka to reach the west coast of India. The numerical experiments therefore raise the possibility that the Bay may have a role in defining the annual cycle of currents in the eastern Arabian Sea.

Not much is known about the currents below the depth of 1000 m in the Arabian Sea. Shetye *et al* (1991c) used current meter records from approximately 1000 and 3000 m at three moorings (16·38 N, 60·50 E; 14·50 N, 64·70 E; and 15·53 N, 68·73 E) during May 1986 to May 1987 to describe the low-frequency currents in the area. It was seen that although the spectra for the six time series had similar shapes, their energies differed. There was no significant coherence between upper and lower currents at any mooring, nor between currents at adjacent moorings. Energies dropped from the west to the east both at the upper and the lower levels, but the drop was much larger in the deeper currents. In fact, the energy in the deeper currents for the periods from 1 to 4 weeks was higher than that at the upper level at the western mooring,

marginally higher at the central mooring, and not significant at the eastern mooring. Shetye *et al* suggested that observed bottom intensification of the currents may be the result of generation of bottom-trapped waves by winds with periods ranging between one and a few weeks. In the open Arabian Sea there does exist a topographic slope (see figure 1) and superimposed on the annual cycle of monsoonal winds are at least two large-scale wind oscillations: quasi-biweekly, first pointed out by Krishnamurti and Balme (1976), and, 40–50 day motions noted by Madden and Julian (1972).

There were some indications in the current meter records that signatures of the annual cycle of wind-forcing appear as deep as 1000 m. For example, the eastward component in the record at 1000 m in the westernmost of the three moorings increased from early May 1986, reached a peak (approximately 5 cm/s) towards the end of July, then decreased and vanished by the end of September. The mean flow during October–December was westward. During January–April it was eastward but weak (about 2 cm/s).

No attempts have been made to reconcile these direct current observations with a picture of large-scale deep and bottom flows derived from water properties. In fact, development of such a picture has only just begun. Warren (1992) has proposed a scheme for circulation of deep and bottom waters in the Arabian Sea. He defines the layer roughly 1500–3500 m deep as the North Indian Deep Water. Below this layer lies the bottom water. Invoking the Stommel and Arons (1960) scheme for global abyssal circulation and using the available estimates of bottom water transport in the N. Indian Ocean, Warren suggests that bottom water upwells in the Arabian Sea at the rate of around $5–10 \times 10^{-5}$ cm/s into the bottom of the North Indian Deep Water layer. Further assuming that the upwelling rate at the top of this layer is less than that at the bottom, and that horizontal flow in the layer is exactly geostrophic, Warren has proposed that the circulation in the layer north of about 10 N consists of a poleward western boundary current and a weaker equatorward flow to the east.

3.2 *Coastal regime*

The coastal belt off India, Pakistan, Oman, Yemen and Somalia constitute the coastal regime of the Arabian Sea. Unlike the west coast of India which forms the eastern boundary of the Arabian Sea, the western boundary is not continuous. It is divided into two parts, the Oman and Yemen coast, and the Somali coast. The Pakistani coast forms the northern boundary. It is short, only about 500 km. Of all these regions, the circulation along the Somali coast during the southwest monsoon is the most energetic. However, as pointed out earlier, this region will not be discussed here.

Using ship-drift data, Shetye and Shenoi (1988) examined the annual cycle of surface currents along the coast of Oman and the west coast of India. They concluded that local winds dominate the coastal currents along the coast of Oman driving an energetic (surface speeds of the order of 50 cm/sec) northeastward current during the southwest monsoon, and a weaker current in the opposite direction during the northeast monsoon. Shetye and Shenoi further concluded that though local winds force the currents along the west coast of India during the southwest monsoon, other mechanisms are important to drive the northeast monsoon coastal current which moves against weak winds.

Recently Shetye *et al* (1990, 1991a) have described the hydrography and circulation along the west coast of India during the southwest and northeast monsoons using hydrographic data collected during the southwest monsoon 1987 and the northeast monsoon 1987–88. During the southwest monsoon (Shetye *et al* 1990) the southernmost part of the west coast of India showed occurrence of upwelling, the near shore surface temperature being lower, by as much as 2·5°C, than farther offshore. There was a shallow (approximately 75 to 100 m deep) equatorward surface current, below which there were signatures of downwelling indicative of a poleward undercurrent hugging the continental slope. $T-S$ characteristics showed that the undercurrent carried low salinity waters found in the south-western Bay of Bengal. Conditions similar to those found at the southern end of the coast were found up to around 15 N; but intensity of upwelling and strength of surface current and undercurrent grew weaker progressively from the south to the north, and ceased to be noticeable at about 20 N. Average width of the surface current was about 150 km, whereas the undercurrent was about 50 km wide. Transport in the equatorward surface current increased from less than $0{\cdot}5 \times 10^6 m^3/s$ to about $4 \times 10^6 m^3/s$ from the northern to the southern end of the west coast. The winds during the period of observation varied between west-northwesterly near the southern end to west-southwesterly near the northern end of the coast. The longshore component of wind stress was generally equatorward. Its magnitude was maximal (0·5 dyn/cm) near the southern end. These observations suggest that during the southwest monsoon the coastal circulation off the west coast of India is dynamically similar to wind-driven eastern boundary currents.

Observations during the northeast monsoon, December 1987 and January 1988, showed the presence of a poleward coastal current that flowed against weak winds (Shetye *et al* 1991a). Near the southern end of the coast, at about 10 N, the current was approximately 400 km wide, 200 m deep and carried the low salinity Equatorial Surface Water. The isopycnals tilted down on approaching the coast. Near the northern end of the coast, at about 22 N, the flow was restricted mainly to the vicinity of the continental slope. The current here was a narrow (100 km), 400 m deep jet with transport of about $7 \times 10^6 m^3/s$. Along most of the coastline a southward moving undercurrent was inferred from the distribution of salinity, temperature and dynamic topography. It appears that the ship-drifts in figure 3 do not do justice to the poleward coastal current, possibly because of two reasons. First, one-degree resolution of the ship-drift data may be too crude to resolve the current. Second, because ship-drifts are influenced by winds in addition to currents, the northeast monsoon coastal current, which moves against winds, might be underestimated. To understand the driving mechanism of the current, Shetye *et al* examined the annual cycle of the contribution of the longshore pressure gradient and that of the winds to the near surface momentum balance using available climatologies. It was seen that the longhsore pressure gradient overwhelmed the winds during the northeast monsoon, whereas during the southwest monsoon the winds dominated. In the Leeuwin Current off western Australia, the only other known eastern boundary current that flows against local winds, the pressure gradient dominates the winds throughout the year. The overall structure of the northeast monsoon coastal current is consistent with that predicted in the analytic model proposed by McCreary *et al* (1986) to explain the Leeuwin Current. In the model a poleward baroclinic pressure gradient is generated by a density gradient along the coast. The latter is known to exist along the west coast of India mainly due to increase in salinity from the southern to northern end of the coast.

Though Shetye *et al* (1990, 1991a) emphasise the role of local forcing – winds during southwest monsoon and density gradient during northeast monsoon – in driving the coastal circulation along the west coast of India, in recent numerical experiments McCreary *et al* (1993) argue that remote forcing can also have considerable impact on the coastal currents along this coast. In their numerical experiments the longshore pressure gradient along the coast during the northeast monsoon resulted from arrival of Kelvin waves from the Bay of Bengal.

The coast of Oman forms the western boundary of the Arabian Sea. But it does not exhibit a remotely forced western boundary current. In a synthesis of available hydrographic data, Brock *et al* (1992) showed that during the southwest monsoon the isopleths in the vicinity of the coast shoal in apparent response to the longshore component of wind stress due to the strong monsoonal jet which dominates the wind field during this season. The shoaling of isopleths is seen over a distance of 150–300 km offshore and extends to depths of 200 to 400 m. Not much is known about the Omani coast during the northeast monsoon. The SST fields derived from satellite-based sensors (Shenoi *et al* 1992) suggest that the northeast monsoon coastal current along the west coast of India may well be turning south along the Omani coast after making its way westward along the coast of Pakistan. There are at present no field observations to support this conjecture. Little is known about the annual cycle of circulation along the coast of Pakistan.

4. Air-sea fluxes and mixed-layer processes

A peculiarity of the annual cycle of SST in the Arabian Sea is the cooling during the northern summer which coincides with the southwest monsoon. Annual march of the SST thus shows four phases (Colborn 1976): (1) a warming phase from approximately February to May; (2) cooling from May to August; (3) warming from September to mid-November; and, (4) cooling from mid-November to January. To identify the processes that control this variability, Shetye (1986) carried out numerical experiments with a Kraus-Turner mixed-layer model to simulate the annual cycle of SST along a zonal strip located at 10 N. Climatology of air-sea fluxes, of horizontal surface drift, etc. were used as input to the model. The main conclusion was that over the open-sea regime surface fluxes of heat and momentum alone simulated reasonably well the SST variability throughout the year except during the May–August (southwest monsoon) cooling phase, when the role of horizontal advection was found important to remove most of the heat gained at the surface during a year. McCreary and Kundu (1989) developed a numerical model which simulated both the thermal field and the advective field over the area north of 10 S and west of 75 E. Their solution demonstrated the importance of coastal upwelling and offshore advection in cooling the western Arabian Sea and the Somali Basin during the southwest monsoon. The model results further suggested that the annual heat and mass budget of the combined area of Somali Basin and the Arabian Sea are closed by equatorial currents: an equatorial undercurrent supplies the cool water that is entrained into the upper layer, and a warm surface equatorial flow transports the entrained water out of the region.

The fact that air-sea heat fluxes dominate the thermodynamics of the surface layer in the Arabian Sea makes it important that we know the variability of these fluxes. An excellent summary of climatologies of the variables which influence evolution of

mixed-layer depth and SST in the N. Indian Ocean has been given by Rao *et al* (1989). They also described monthly mixed layer depth, SST and surface current climatologies.

In a recent study Bauer *et al* (1991) have shown how air-fluxes of heat and momentum can together lead to a peculiarity of the Arabian Sea thermal field: during the south-west monsoon the depth of mixed-layer in the Arabian Sea varies with latitude with shallowest depths occurring under the region of maximum winds and the maximum depths to the south. By examining the influence of northeast 1986, 1987 and southwest 1987 monsoon on surface layers of the Arabian Sea, Bauer *et al* showed that this feature can be linked to the Ekman flow induced by the wind stress. To the north of the monsoon jet the Ekman flow is such that there is a net divergence of transport. As a result, the fluid below the seasonal thermocline upwells, thus suppressing development of mixed-layer. Convergence of Ekman transport in the area south of the wind maximum deepens the seasonal thermocline leading to warmer temperatures. The important result here is that, consistent with the conclusions of Hastenrath and Greischar (1991), structure of the near surface velocity and thermal fields in the Arabian Sea can be understood using simple ideas of wind-driven Ekman flow and slab-mixed-layers.

5. Water masses

Annual precipitation over the Arabian Sea varies from less than 0·1 m in the northern and western parts to 2 m in the southern part. The south-eastern part of the sea is in contact with the Bay of Bengal and the eastern equatorial Indian Ocean where precipitation is about 2 m/year. Average annual evaporation over the Arabian Sea is uniform, about 1·5 m. As a result, the Arabian Sea as a whole loses water to the atmosphere and a distinct gradient exists in the field of precipitation minus evaporation. The western and northern parts lose, on average, more than 1·0 m annually. Only the southeastern corner gains water. This gradient in precipitation minus evaporation leads to a gradient in surface salinity with higher salinity in the north. During the northeast monsoon continental winds cool the surface of the northern Arabian Sea, most notably its north-eastern corner. The net result of the high salinity and the northeast monsoon cooling is formation of water that has σ_θ in the range 24–25. This is higher than surface densities found anywhere else in the N. Indian Ocean except the mediterranean basins. The high salinity water that forms at surface in the N. Arabian Sea has been called the Arabian Sea High Salinity Water (ASHSW). High precipitation in the southern and eastern parts of the N. Indian Ocean, on the other hand, leads to formation of the Equatorial Surface Water (Darbyshire 1967) which is generally found in upper 50–75 m and in which salinity increases with depth. This water moves into the Arabian Sea during the northeast monsoon either with the surface drift over open-sea or with the current along the coast of India. On confluence of the high salinity water of northern origin and low salinity water of southern origin, the former sinks below the latter, leading to formation of a sub-surface salinity maximum which marks the core of the ASHSW (Rochford 1964).

A horizontal salinity gradient is also found at subsurface depths in the Arabian Sea due to the influence of two mediterranean basins, the Persian Gulf and the Red Sea. Average depth of the Persian Gulf is 25 m and evaporation at surface exceeds

precipitation by about 2 m annually. This leads to formation of a warm saline water mass, the Persian Gulf Water (PGW), which flows into the Gulf of Oman at depths of 25 to 70 m through the straits of Hormuz. In the Gulf of Oman the water sinks to depths between 200 and 250 m. Spread of this water in the northern Arabian Sea leads to formation of a salinity maximum which is found between 200 and 400 m with deeper depths to the south. In the Red Sea too evaporation exceeds precipitation by over 2 m/year. The resulting Red Sea Water (RSW) flows over the 110 m sill at the Strait of Bab el Mandeb to enter the Gulf of Aden at 36 ppt and 15°C (Pickard and Emery 1982). Spread of this water in the Arabian Sea leads to a salinity maximum. The northern extent of this maximum is marked approximately by 18 N, and its depth changes from about 500 m in the north to about 800 m near the equator. Figures 7(a–c) show the regions where the three maxima (ASHSW, PGW and RSW) are found and the salinities at these maxima. The annual files of Levitus (1982) atlas have been used to prepare these figures.

The water mass between about 100 and 800 m depth in the western equatorial N. Indian Ocean has often been called the Indian Ocean Equatorial Water (Sverdrup *et al* 1942). It is formed from mixture of the Indian Central Water and the Australasian Mediterranean Water, both of which form south of the equator (You and Tomczak 1993). Characteristics of the waters in upper 1000 m in the Arabian Sea are the result of mixture of the ASHSW, PGW and RSW, the three waters that form in the Arabian Sea, with the Indian Ocean Equatorial Water. In addition, the Equatorial Surface Water is often found at the surface.

According to the scheme for circulation of deep and bottom waters put forth by Warren (see section 3.2), the bottom water of the Arabian Sea is derived from south of the equator. At 4000 m in the Arabian Sea salinity varies between 34·730–34.737 ppt, and potential temperature between 1·090–1·330°C. At 2500 m, mid-depth of the Indian

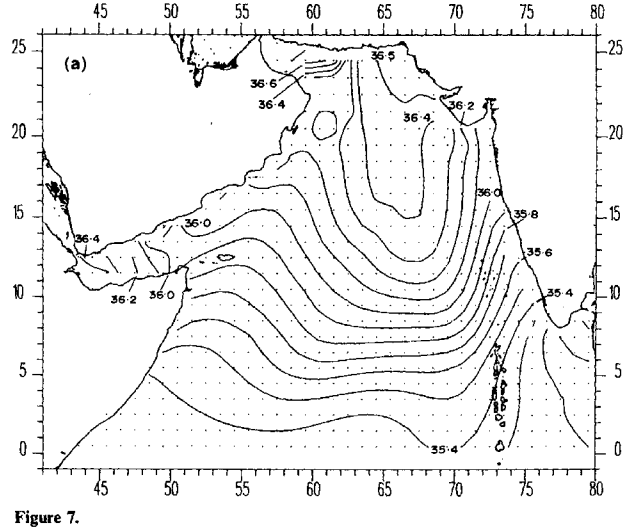

Figure 7.

Figure 7. (*Continued*).

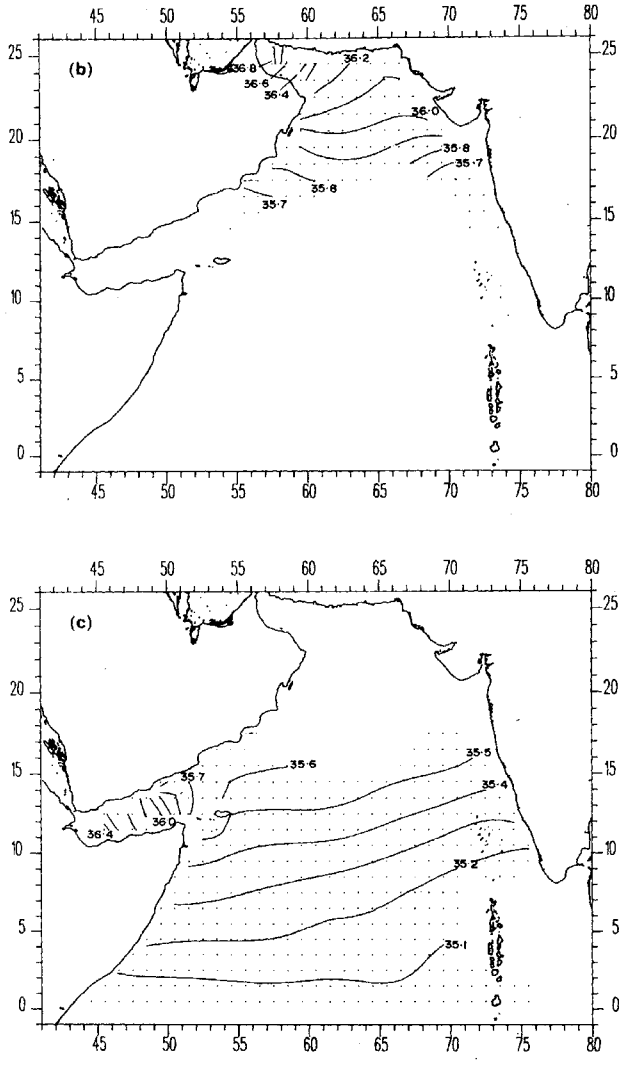

Figure 7. Distribution of salinity (ppt) in the maximum due to (a) Arabian Sea High Salinity Water; (b) Persian Gulf Water; and, (c) Red Sea Water. A dot at a location implies that the maximum is found at the location. The annual mean data file on temperature and salinity from Levitus (1982) atlas was used to prepare the figures.

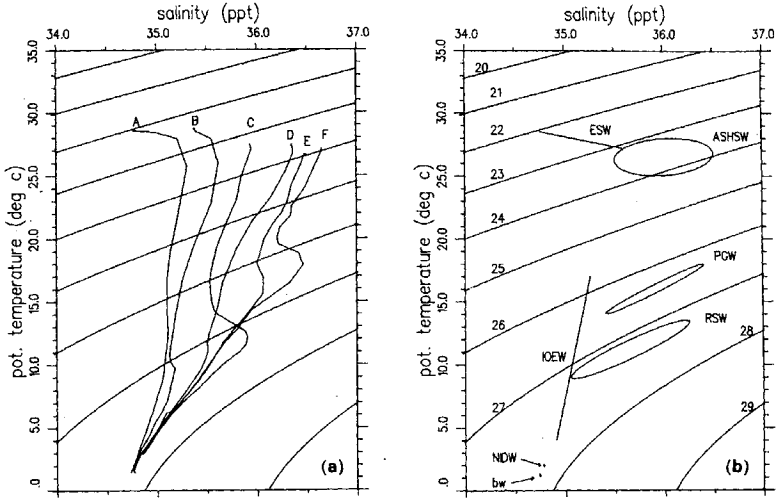

Figure 8(a). Potential temperature-salinity curves using Levitus (1982) annual mean data from a few locations in the Arabian Sea. **A**: 4·5 N 74·5 E; **B**: 5·5 N 65·5 E; **C**: 13·5 N 49·5 E; **D**: 14·5 N 65·5 E; **E**: 22·5 N 65·5 E; **F**: 24·5 N 59·5 E. Solid lines are contours of equal potential density.

Figure 8(b). Potential temperature-salinity diagram of water masses found in the Arabian Sea. The ellipses show approximate range of potential temperature and salinity found in the maxima due to Arabian Sea High Salinity Water (ASHSW), Persian Gulf Water (PGW) and Red Sea Water (RSW). ESW represents the layer of Equatorial Surface Water in which salinity increases with depth. The surface and the bottom salinity of this layer can vary considerably with location. "NIDW" and "bw" show characteristics of, respectively, the North Indian Deep Water and the water found at depth of about 4000 m in mid-Arabian Sea. Also shown are contours of equal potential density.

Deep Sea Water layer, θ and S range is 1·910–2·109°C and 34·769–34·783 ppt respectively (see average properties in the 300-mile squares given in Wyrtki 1971). As the bottom water upwells in the Arabian Sea, it is transformed – salinity and temperature increased, dissolved oxygen decreased – into the North Indian Deep Water (1500–3500 m). Figure 8(a) gives a few examples of $\theta - S$ curves observed in the Arabian Sea. Figure 8(b) provides a summary of $\theta - S$ signatures of the water masses that are useful to put into perspective the observed curves.

6. Concluding comments

In conclusion, the dynamics and thermodynamics of the surface layer of the Arabian Sea are reasonably well understood and can be linked to the annual cycle of air-sea fluxes due to the monsoons. The more intriguing aspect of the circulation of this Sea is the subsurface flow. There is some evidence that the annual cycle of Ekman suction

plays a role in seasonality of these currents, particularly in the western and central parts of the sea. A new theory that has evolved from the results of recent numerical experiments (McCreary *et al* 1993; Potemra *et al* 1991) is that subsurface reversal of the currents in eastern Arabian Sea is largely the result of the Rossby waves radiated by the Kelvin waves propagating along the west coast of India. Arabian Sea, being a tropical basin which experiences a distinctly time-dependent forcing, is one of the few regions of the world oceans (possibly, the only other is the Bay of Bengal) where this mechanism can play a dominant role. Proximity of the N. Indian basin to the equator makes it possible for westward propagating equatorial Rossby waves to serve as fast carriers of energy from an eastern boundary to interior of the basin. Observations are needed to examine this possibility. If found true it would open new possibilities on how the Arabian Sea and the North Indian Ocean work. Little is known at present about the deep and the bottom water circulation in the Arabian Sea, and the ideas developed by Warren (1982) need to be scrutinised with field data.

Acknowledgements

The British Oceanographic Data Centre, Proudman Oceanographic Laboratory, Bidston, made available the Cutler and Swallow (1984) atlas in digital form.

References

Bauer J G, Hitchcock G L and Olson D B 1991 Influence of monsoonally-forced Ekman dynamics upon surface layer depth and plankton biomass distribution in the Arabian Sea; *Deep Sea Res.* **38** 531–553

Breidenbach J 1990 EOFs of pseudo-stress over the Indian Ocean (1977–85); *Bull. Am. Meteor. Soc.* **13** 1443–1454

Brock J C, McClain C R and Hay W W 1992 A southwest monsoon hydrographic climatology for the northwestern Arabian Sea; *J. Geophys. Res.* **97** 9455–9465

Colborn J 1976 The thermal structure of the Indian Ocean, (Hawaii: The University Press of Hawaii) pp. 173

Cutler A N and Swallow J C 1984 Surface currents of the Indian Ocean (To 25 S, 100 E): compiled from historical data archived by the Meteorological Office, (Bracknell, UK: Institute of Oceanographic Sciences, Wormley, Report No. 187, 36 charts) pp. 8

Darbyshire M 1967 The surface waters off the coast of Kerala, south-west India; *Deep Sea Res.* **14** 295–320

Duing W 1970 The monsoon regime of the currents in the Indian Ocean, (Honolulu: East-West Center Press) Contribution No. 330 from the Hawaii Institute of Geophysics, University of Hawaii, pp. 68

Hastenrath S and Greischar L 1991 The monsoonal current regimes of the tropical Indian Ocean: observed surface flow fields and their geostrophic and wind-driven components; *J. Geophys. Res.* **96** 12619–12633

Hellermann S and Rosenstien M 1983 Normal wind stress over the world ocean with error estimates; *J. Phys. Oceanogr.* **13** 1093–1104

Krishnamurti T N and Balme H N 1976 Oscillations of a monsoon system. Part 1 – observational aspects; *J. Atmos. Sci.* **33** 1937–1954

Levitus S 1982 Climatological Atlas of the World Ocean, (Washington DC: U.S. Department of Commerce) NOAA Professional paper 13, pp. 173

Luther M E and O'Brien 1985 Modelling the variability of the Somali Current. In: *Coherent structures in geophysical turbulence*, (ed) J C Nihoul (New York: Elsevier)

Madden R A and Julian P R 1972 Description of global scale circulation cells in the tropics with 40–50 day period; *J. Atmos. Sci.* **29** 1109–1123

McCreary J P Jr. and Kundu P K 1989 A numerical investigation of sea surface temperature variability in the Arabian Sea; *J. Geophys. Res.* **94** 16097–16114

McCreary J P Jr., Shetye S R and Kundu P K 1986 Thermohaline forcing of eastern boundary currents: With application to the circulation off the west coast of Australia; *J. Mar. Res.* **44** 71–92

McCreary J P Jr., Kundu P K and Molinari R L 1993 A numerical investigation of dynamics, thermodynamics and mixed-layer processes in the Indian Ocean; *Prog. Oceanogr.* **31** 181–244

Murty V S N, Sarma Y V B, Rao D P and Murty C S 1992 Water characteristics, mixing and circulation in the Bay of Bengal during southwest monsoon; *J. Mar. Res.* **50** 207–228

Pickard G L and Emery W J 1982 Descriptive physical oceanography: an introduction, 4th ed., (Oxford: Pergamon Press) pp. 249

Potemra J T, Luther M E and O'Brien J J 1991 The seasonal circulation of the upper ocean in the Bay of Bengal; *J. Geophys. Res.* **96** 12667–12683

Rao R R, Molinari R L and Festa J F 1989 Evolution of the climatological near-surface thermal structure of the tropical Indian Ocean. Part-1: Description of mean monthly mixed-layer depth and sea-surface temperature, surface current and surface meteorological fields, *J. Geophys. Res.* **94** 10801–10815

Robinson M K 1966 Arabian Sea. In: *Encyclopaedia of earth sciences series, volume 1: The Encyclopaedia of Oceanography* (ed) R W Fairbridge (Stroudsburg, Pennsylvania: Dowden, Hutchinson & Ross, Inc.) pp. 40–44

Rochford D J 1964 Salinity maxima in the upper 1000 meters of the North Indian Ocean; *Aust. J. Mar. Freshwater Res.* **15** 1–24

Schott F 1983 Monsoon response of the Somali current and associated upwelling; *Prog. Oceanogr.* **12** 357–381

Shenoi S S C, Gouveia A D, Shetye S R and Rao L V G 1992 Satellite observations of the northeast monsoon coastal current. In: *Proceedings of the PORSEC-'92 in Okinawa, Vol. 2*, (Shimizu, Shizuoka: PORSEC Secretariat) pp. 796–801

Shetye S R 1986 A model study of the seasonal cycle of the Arabian Sea surface temperature; *J. Mar. Res.* **44** 521–542

Shetye S R and Shenoi S S C 1988 The seasonal cycle of surface circulation in the coastal North Indian Ocean; *Proc. Indian Acad. Sci. (Earth Planet. Sci.)* **97** 53–62

Shetye S R, Gouveia A D, Shenoi S S C, Sundar D, Michael G S, Almeida A M and Santanam K 1990 Hydrography and circulation off the west coast of India during the Southwest Monsoon 1987; *J. Mar. Res.* **48** 359–378

Shetye S R, Gouveia A D, Shenoi S S C, Michael G S, Sundar D, Almeida A M and Santanam K 1991a The coastal current off western India during northeast monsoon; *Deep Sea Res.* **38** 1517–1529

Shetye S R, Shenoi S S C, Gouveia A D, Michael G S, Sundar D and Nampoothiri G 1991b Wind-driven coastal upwelling along the western boundary of Bay of Bengal during southwest monsoon; *Con. Shelf Res.* **11** 1397–1408

Shetye S R, Shenoi S S C and Sundar D 1991c Observed low frequency currents in the deep mid-Arabian Sea; *Deep Sea Res.* **38** 57–65

Shetye S R, Gouveia A D, Shenoi S S C, Sundar D, Michael G S and Nampoothiri G 1993 The western boundary current of the seasonal subtropical gyre in the Bay of Bengal; *J. Geophys. Res.* **98** 945–954

Stommel H and Arons A B 1960 On the abyssal circulation of the world ocean – I. Stationary planetary flow patterns on a sphere; *Deep Sea Res.* **6** 140–154

Sverdrup H U, Johnson M W and Fleming R H 1942 The Oceans, (Englewood Cliffs, N.J.: Prentice-Hall, Inc.) pp. 1087

Warren B A 1992 Circulation of north Indian deep water in the Arabian Sea. In: *Oceanography of the Indian Ocean* (ed) B N Desai (New Delhi: Oxford & IBH Publishing Co.) pp. 575–582

Wyrtki K 1971 Oceanographic atlas of the International Indian Ocean Expedition, (Washington DC: U.S. Government Printing Office) pp. 531

Wyrtki K 1973 Physical Oceanography of the Indian Ocean; In: *The Biology of the Indian Ocean* (ed) B Zeitzschel and S A Gerlach (London: Chapman and Hall Ltd) pp. 18–36

You Y and Tomczak M 1993 Thermocline circulation and ventilation in the Indian Ocean derived from water mass analysis; *Deep Sea Res.* **40** 13–56

Yu L, O'Brien J J and Yang J 1991 On the remote forcing of the circulation in the Bay of Bengal; *J. Geophys. Res.* **96** 20449–20454